Biochemistry

 Volume 40, Number 22 June 5, 2001

Accelerated Publications

Structure of the Transmembrane Dimer Interface of Glycophorin A in Membrane Bilayers†

Steven O. Smith,*,‡ David Song,§ Srinivasan Shekar,‡,§ Michel Groesbeek,§ Martine Ziliox,‡ and Saburo Aimoto||

Department of Biochemistry and Cell Biology, Center for Structural Biology, State University of New York at Stony Brook, Stony Brook, New York 11794-5115, Department of Molecular Biophysics and Biochemistry, Yale University, New Haven, Connecticut 06520, and Institute for Protein Research, Osaka University, Osaka, Japan

Received February 20, 2001; Revised Manuscript Received March 29, 2001

ABSTRACT: The hydrophobic transmembrane domain of glycophorin A contains a sequence motif that mediates dimerization in membrane environments. Long-range interhelical distance measurements using magic angle spinning NMR spectroscopy provide high-resolution structural constraints on the packing of the dimer interface in membrane bilayers. We show that direct packing contacts occur between glycine residues at positions 79 and 83 in the transmembrane sequence. Additional interhelical constraints between Ile76 and Gly79 and between Val80 and Gly83 restrict the rotational orientation and crossing angle of the interacting helices. These results refine our previously proposed structure of the glycophorin A dimer [Smith, S. O., and Bormann, B. J. (1995) *Proc. Natl. Acad. Sci. U.S.A. 92*, 488−491] which revealed that the methyl groups of Val80 and Val84 are packed against Gly79 and Gly83, respectively.

Helix−helix interactions are important in the folding and function of membrane proteins with multiple membrane spanning helices (*1*). In proteins with single membrane spanning helices, helix−helix interactions are often involved in guiding protein oligomerization and can serve as determinants for protein localization or internalization. Over the past few years, high-resolution structures of polytopic membrane proteins have provided the first insights into how hydrophobic transmembrane helices associate in membrane environments. One of the striking observations has been that residues with small side chains (Gly, Ala, Thr, Ser) frequently mediate tight helix−helix contacts (*2*, *3*).

The transmembrane domain of glycophorin A provides a simple system for understanding the structural basis for helix association. Bormann and Marchesi originally showed that the single transmembrane helix of glycophorin A was responsible for protein dimerization (*4*). The first clear evidence for the dimer interface came from the mutational studies of Engelman and co-workers (*5*, *6*). They demonstrated that a seven-residue motif is involved in dimerization (Figure 1). The mutational results were placed into the context of a dimer model by Treutlein et al. (*7*) using molecular dynamics calculations. Their model exhibited close Gly79−Gly79 and Gly83−Gly83 packing interactions. However, valine residues at positions 80 and 84 identified as part of the dimerization motif were oriented away from the dimer interface. Solid-state magic angle spinning (MAS)[1] NMR measurements provided evidence that these valine side chains were packed against glycine residues on the opposing helix in the dimer (*8*). The strongest contacts were found between

† This work was supported in part by a grant to S.O.S. from the National Institutes of Health (GM-46732).

* To whom correspondence should be addressed. Telephone: 631-632-1210. Telefax: 631-632-8575. E-mail: steven.o.smith@sunysb.edu.

‡ State University of New York at Stony Brook.

§ Yale University.

|| Osaka University.

10.1021/bi010357v CCC: $20.00
Published on Web 05/10/2001

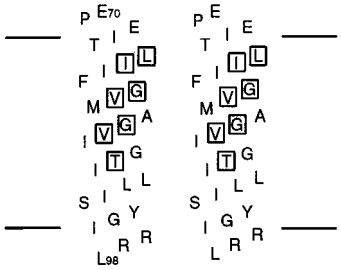

FIGURE 1: Transmembrane sequence of glycophorin A from Glu70 to Leu98. The seven residues which mediate dimerization of the transmembrane helices are boxed.

Val80 and Gly79 and between Val84 and Gly83. More recently, Mackenzie et al. (*9*) undertook solution NMR studies of the glycophorin A transmembrane dimer in detergent micelles. The observation of five NOE ^{1}H−^{1}H correlations that were not generated from intramonomer contacts provided a basis for modeling the dimer interface. Their structure was consistent with the prior MAS NMR measurements showing Val−Gly contacts but did not exhibit direct Gly−Gly contacts.

The relatively small number of structural constraints from both solution and solid-state NMR studies has left open the question of the detailed rotational orientation of the helices and the specific packing interactions in the dimer interface. The importance of glycine interactions in helix−helix packing in polytopic membrane proteins has recently been highlighted by detailed analyses of the packing of transmembrane helices in known crystal structures of membrane proteins (*2*, *3*). The unexpected result from these studies was the high occurrence of glycine in helix interfaces. In this study, rotational resonance NMR measurements provide high-resolution constraints on how the glycine residues contribute to the detailed packing of the glycophorin A dimer interface.

MATERIALS AND METHODS

Lipids were obtained as lyophilized powders from Avanti Polar Lipids (Alabaster, AL). Isotopic ^{13}C-labeled amino acids were obtained from Cambridge Isotope Laboratories (Andover, MA) or Mass Trace (Woburn, MA).

Synthesis, Purification, and Reconstitution of Glycophorin A Transmembrane Peptides. Peptides (29 residues in length) corresponding to the transmembrane domain of human glycophorin A were synthesized using solid-phase methods. The sequence is shown in Figure 1. The peptides were purified by reverse-phase HPLC as follows. Crude peptide (5−15 mg) was dissolved in 1 mL of trifluoroacetic acid (TFA), injected onto a reverse-phase C4 or C18 HPLC column, and purified by gradient elution using distilled (Millipore) water (solvent A), 95% acetonitrile (solvent B), and 95% 2-propanol (solvent C). The C18 column has better resolution, but a lower yield of protein. The initial aqueous solvent conditions (70% solvent A, 12% solvent B, 18% solvent C) were gradually changed to a more hydrophobic composition (40% solvent B, 60% solvent C) where the peptides elute. The elution was monitored by the optical absorbance at 280 nm. The solutions corresponding to the peaks were collected into several fractions. The fractions were then lyophilized and checked by mass spectrometry for purity.

Purified glycophorin A peptides were reconstituted by detergent dialysis. A comprehensive study of membrane reconstitution of glycophorin A transmembrane peptides showed that the most robust method for obtaining homogeneous reconstitutions of peptides in transmembrane orientations was by dialysis from octyl β-glucoside followed by sucrose gradient purification (S. O. Smith, D. Song, W. Liu, E. Crocker, S. Shekar, M. Eilers, W. Ying, G. Metz, M. Ziliox, and S. Aimoto, submitted for publication). Briefly, lipid (DMPC or POPC), peptide (lyophilized), and detergent (octyl β-glucoside) were dissolved in trifluoroethanol. The trifluoroethanol was removed by evaporation using a stream of argon gas and then placing under vacuum. The dry lipid/peptide/detergent mixture was rehydrated with phosphate buffer (10 mM phosphate and 50 mM NaCl, pH 7), such that the final concentration of octyl β-glucoside was 5% (w/v). The rehydrated sample was then stirred slowly for at least 6 h, and the octyl β-glucoside was removed by dialysis using Spectra-Por dialysis tubing (3500 MW cutoff) for 24 h against phosphate buffer at a temperature above the lipid phase transition. The resulting membrane vesicles were sonicated and loaded onto a 10%−40% (w/v) sucrose gradient and ultracentrifuged at 150000*g* for 8−12 h at 5 °C (POPC) or 15 °C (DMPC). Generally, the reconstituted membranes formed two discrete bands in the sucrose gradient. For NMR measurements, we used the upper band which had a more homogeneous appearance and a higher lipid:peptide ratio (40:1−60:1) as assessed by FTIR analysis. The sucrose was removed by dialysis against phosphate buffer for 24 h. The reconstituted membranes were then pelleted to form multilamellar dispersions and loaded into NMR rotors.

Magic Angle Spinning NMR. MAS NMR measurements were made on a Chemagnetics or Bruker Avance 360 MHz spectrometer using double resonance probes from Doty Scientific (Columbia, SC) or Chemagnetics (Fort Collins, CO). ^{13}C spectra were acquired with ramped amplitude (*10*) proton cross-polarization (CP) and with single pulse excitation. TPPM proton decoupling was employed during ^{13}C acquisition (*11*). Typically, the ^{1}H and ^{13}C pulse lengths were ∼3−4 μs, with a CP contact time of 3 ms and a recycle delay of 2.5 s. The proton decoupling field strengths were generally ∼83 kHz. Signals were averaged in blocks of 1024 or 2048 transients. The time domain signals were zero filled to 2048 or 4096 points and typically multiplied by a 15 Hz line-broadening function before Fourier transformation.

The experimental design of the rotational resonance experiment has been described previously (*12*). The rotational resonance pulse sequence begins with ^{1}H−^{13}C cross-polarization to generate ^{13}C polarization that is then stored on the *Z* axis with a ^{13}C flip-back pulse. One of the two ^{13}C resonances is selectively inverted with a low-power 500 μs pulse, and magnetization is allowed to exchange between the two sites for a variable mixing period. The power level of the inversion pulse is carefully adjusted to yield the maximum inversion. The distribution of ^{13}C signal at the end of the mix period is detected with a 90° pulse that flips

[1] Abbreviations: DMPC, dimyristoylphosphocholine; MAS, magic angle spinning; NMR, nuclear magnetic resonance; NOE, nuclear Overhauser enhancement; POPC, 1-palmitoyl-2-oleoylphosphocholine; TFA, trifluoroacetic acid.

the magnetization into the transverse plane for acquisition of the NMR signal.

RESULTS AND DISCUSSION

Rotational Resonance NMR of Known Distances in a Transmembrane Helix. Quantitative measurements of dipolar couplings using rotational resonance require calibrations with model compounds to establish an effective zero quantum T_2 relaxation parameter. Our previous studies on Val···Gly packing relied on calibration of $^{13}CH_3\cdots{}^{13}C{=}O$ distance measurements using crystalline alamethicin model peptides bearing a series of labeled $^{13}CH_3\cdots{}^{13}C{=}O$ spin pairs at known distances (*12*). Since Gly−Gly distance measurements involve $^{13}CH_2\cdots{}^{13}C{=}O$ rather than $^{13}CH_3\cdots{}^{13}C{=}O$ pairs, we first describe rotational resonance measurements on glycophorin peptides incorporating a $^{13}CH_3\cdots{}^{13}C{=}O$ pair at a known intrahelical distance and compare this to intrahelical measurements on a $^{13}CH_2\cdots{}^{13}C{=}O$ pair. Our previous work on the decoupling dependence of rotational resonance recoupling (*12*) argued that a CH_2 group has a shorter effective zero quantum T_2 relaxation time than a CH_3 group since the $^{13}C-{}^{1}H$ dipolar coupling is weaker for a methyl group due to fast methyl group rotation. In this section, we compare rotational resonance NMR curves of the glycophorin A transmembrane domain labeled at 1-^{13}C-Phe78 and 3-^{13}C-Ala82 with rotational resonance curves from glycophorin A labeled at 1-^{13}C-Val80 and 2-^{13}C-Gly83. These peptides incorporate labeled $^{13}CH_3\cdots{}^{13}C{=}O$ and $^{13}CH_2\cdots{}^{13}C{=}O$ spin pairs that span one turn of an α-helix. The average intrahelical distance between a carbonyl carbon at residue i and an α-carbon at residue $i + 3$ is ∼4.5 Å, while the distance between a carbonyl carbon and an β-carbon at residue $i + 4$ is ∼4.6 Å.

Figure 2a presents the rotational resonance magnetization exchange curve at −10 °C for the glycophorin A transmembrane peptide bearing single labels at 1-^{13}C-Phe78 and 3-^{13}C-Ala82. In these experiments, the $^{13}C{=}O$ resonance at ∼175 ppm was inverted with a low-power selective pulse, and the MAS frequency was controlled at 14.554 kHz. This frequency corresponds to the $n = 1$ resonance condition and equals the spacing between the two ^{13}C resonances. A series of spectra were collected as a function of the rotational resonance mixing time during which magnetization is exchanged between the two dipole-coupled spins. The intensity changes which are observed in the coupled $^{13}C{=}O$ and $^{13}CH_3$ resonances are plotted as a function of the exchange time and are related to the strength of the dipole coupling and internuclear distance. Assuming a standard α-helical distance of 4.6 Å, the experimental data are best simulated with a zero quantum T_2 relaxation time of 1.6 ms. This value of the zero quantum relaxation time is significantly shorter than that previously determined for crystalline alamethicin peptides (*12*) as would be expected for membrane reconstituted peptides having larger line widths and was used to simulate interhelical Val $^{13}CH_3\cdots$Gly $^{13}C{=}O$ $n = 1$ rotational resonance measurements (data not shown).

Figure 2b presents rotational resonance magnetization exchange curves for the glycophorin A transmembrane peptide bearing single labels at 1-^{13}C-Val80 and 2-^{13}C-Gly83. In this case, the experimental data are best simulated with a zero quantum T_2 relaxation time of 1.4 ms based on an intrahelical distance of 4.5 Å. The 1.4 ms relaxation time is slightly less than found above for the $^{13}CH_3\cdots{}^{13}C{=}O$ spin pair as would be expected due to the stronger $^{1}H-{}^{13}C$ dipolar coupling in the methylene group of 2-^{13}C-Gly83. In Figure 2c, the data for the $^{13}CH_2\cdots{}^{13}C{=}O$ experiment are plotted

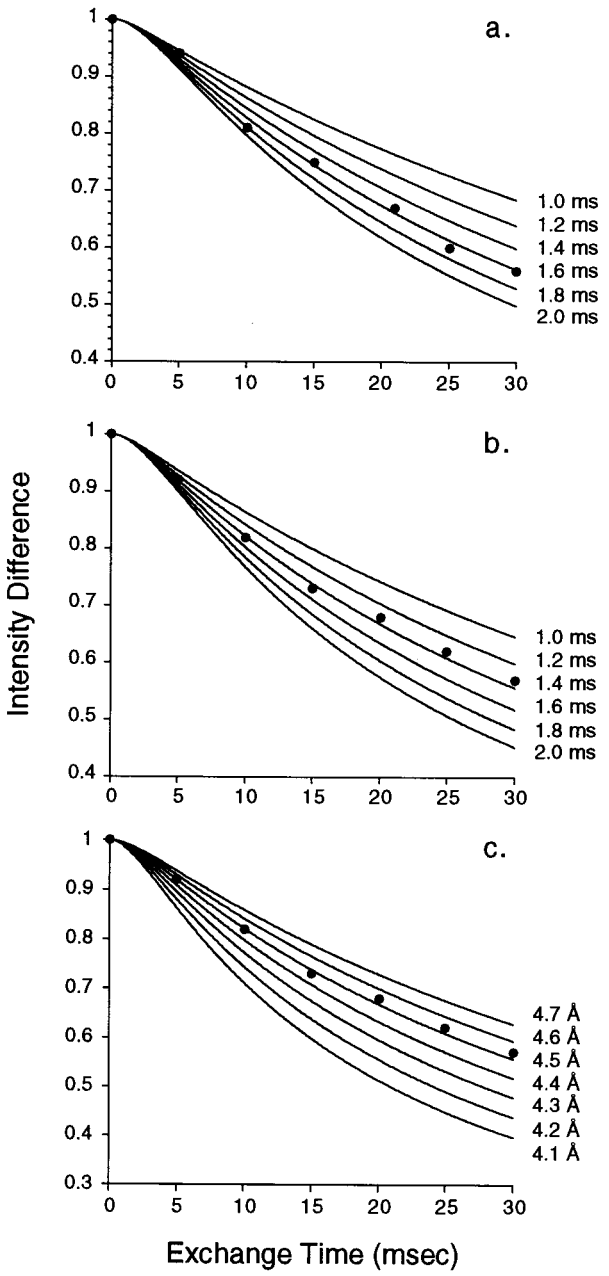

FIGURE 2: Intrahelical rotational resonance distance measurements. (a) Rotational resonance magnetization exchange curve and simulations for the glycophorin A transmembrane peptide labeled at both 1-^{13}C-Phe78 and 3-^{13}C-Ala82 reconstituted into DMPC multilayers. Spectra were obtained at 14.554 kHz, the $n = 1$ resonance condition. The proton decoupling field was 83 kHz. Simulations are shown using a dipolar coupling of 78 Hz (4.6 Å) and varying the zero quantum T_2 parameter from 1.0 to 2.0 ms. (b) Rotational resonance magnetization exchange curve and simulations for glycophorin A labeled at 1-^{13}C-Val80 and 2-^{13}C-Gly83 reconstituted into DMPC multilayers. Spectra were obtained at 11.824 kHz, the $n = 1$ resonance condition. Simulations are shown using a dipolar coupling of 83 Hz (4.5 Å) and varying the zero quantum T_2 parameter from 1.0 to 2.0 ms. (c) Rotational resonance exchange data for 1-^{13}C-Val80 and 2-^{13}C-Gly83 are shown as in (b) but simulated with a zero quantum T_2 of 1.4 ms and varying the dipolar coupling from 73 Hz (4.7 Å) to 110 Hz (4.1 Å).

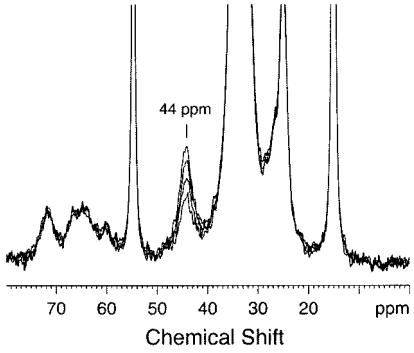

FIGURE 3: Interhelical rotational resonance distance measurements. Rotational resonance spectra of the $^{13}CH_2$ region of glycophorin A. Spectra are shown that were obtained with mixing times of 100 μs and 5, 10, and 30 ms. The resonances that are "off" of the rotational resonance condition do not change in intensity.

along with simulations in which the zero quantum T_2 relaxation time is held fixed at 1.4 ms and the internuclear distance is varied from 4.1 to 4.7 Å. This illustrates that the precision in the measurements is on the order of ±0.1 Å. These data provide a simple way to internally calibrate the measurements of unknown distances in reconstituted glycophorin A peptides. The 1.4 ms zero quantum T_2 relaxation time is used in the simulations of interhelical measurements described below.

Packing of Gly79 and Gly83 in the Dimer Interface of Glycophorin A. The strategy we have taken to establish structural constraints for the interfacial packing of the glycophorin A dimer is to measure direct dipolar interactions in MAS NMR experiments using rotational resonance techniques. Single ^{13}C-labeled sites in glycophorin A peptides are incorporated synthetically, and peptides containing unique labels are combined in membrane reconstitutions. The dipolar coupling has an r^{-3} distance dependence, and the direct measurement of the dipolar coupling in a MAS experiment can provide longer range distance constraints with greater accuracy than is possible in solution NMR using NOE techniques that have an r^{-6} distance dependence. In the experiments described below, the $^{13}CH_2$ and $^{13}C{=}O$ labeled peptides were reconstituted in a 1:4 molar ratio. The $^{13}CH_2$ resonance is selectively observed as the glycine α-carbon does not overlap with other protein resonances. The 1:4 dilution results in 71% of the $^{13}CH_2$-labeled peptide forming heterodimers with $^{13}C{=}O$ labeled peptide, assuming quantitative dimerization of the transmembrane domain. In detergent micelles, the dissociation constant of helix dimers has been measured as 240 nm using analytical ultracentrifugation (*13*) and as 80 nm using FRET (*14*) and is dependent on the nature of the detergent. The tightest dimers are formedin zwitterionic detergents (*14*) which provide a more membrane-like environment. The assumption of quantitative dimerization is supported by simultaneously fitting of the CH_2 (this paper) and CH_3 (*8*) distance measurements using the zero quantum T_2 values based on the known intrahelical distances. Importantly, a distribution of monomers and dimers would lead to shorter, rather than longer, internuclear distances than calculated below.

Figure 3 presents the upfield region containing the Cα carbon resonance of Gly79. In this case, glycophorin A peptides ^{13}C-labeled at the α-carbon of Gly79 were reconstituted in a 1:4 ratio with peptides ^{13}C-labeled at the carbonyl

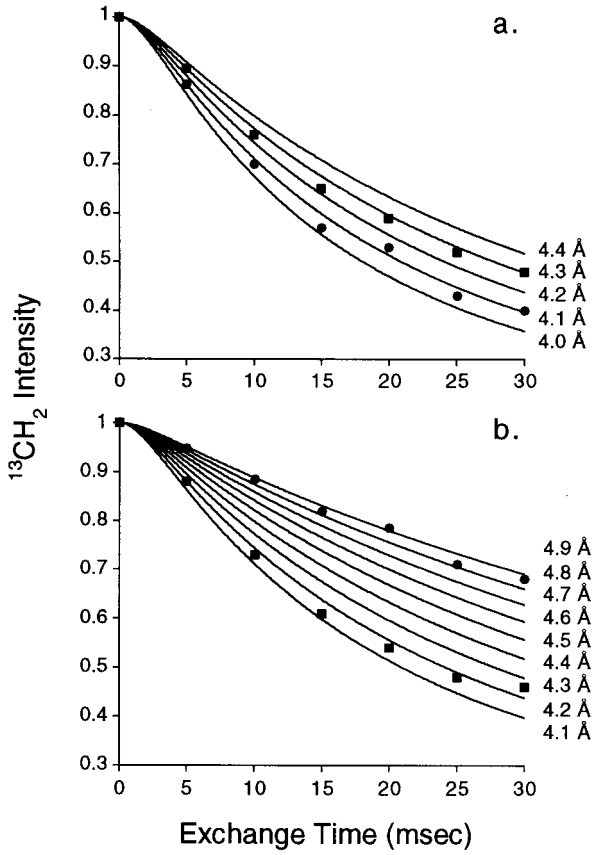

FIGURE 4: Interhelical rotational resonance distance measurements. Rotational resonance exchange curves and simulations for interhelical distances in the glycophorin A dimer. Glycophorin A peptides were reconstituted in a 1:4 molar ratio with labels at (a) 2-^{13}C-Gly79 and 1-^{13}C-Gly79 (circles), 2-^{13}C-Gly83 and 1-^{13}C-Gly83 (squares) and (b) 2-^{13}C-Gly79 and 1-^{13}C-Ile76 (circles), 1-^{13}C-Val80 and 2-^{13}C-Gly83 (squares). The rotational resonance exchange curves are simulated with a zero quantum T_2 of 1.4 ms and varying the dipolar coupling from 73 Hz (4.7 Å) to 110 Hz (4.1 Å). The rotational resonance curves have been corrected for off-rotational resonance decay (8% at 30 ms) and 29% nonexchanging 2-^{13}C-Gly labeled peptide that has formed homodimers. Rotational resonance measurements of the glycophorin A dimers in DMPC and POPC gave similar results.

carbon of Gly79. The carbonyl resonance at 175 ppm has been inverted, and only the intensity of the Cα resonance at 44 ppm is monitored as a function of the rotational resonance exchange time. The exchange spectra shown are scaled to minimize the differences of off-rotational resonance peaks.

Figure 4 presents rotational resonance data and simulated exchange curves for four independent experiments. The $^{13}CH_2{\cdots}^{13}C{=}O$ measurements across the dimer interface are shown for Gly79−Gly79 (filled squares) and Gly83−Gly83 (filled circles) in Figure 4a. The short (~4.2 Å) internuclear distance is consistent with direct Gly−Gly packing. Figure 4b presents $^{13}CH_2{\cdots}^{13}C{=}O$ measurements between backbone labels at Gly79 and Val80 (squares) and Gly83 and Ile76 (circles). These measurements help to restrict the rotational orientation of the helices in the dimer.

The structural restraints derived from the rotational resonance NMR experiments are summarized in Table 1. These restraints along with those previously obtained on Val−Gly interactions (*8*) were used to refine our model of the dimer interface presented in Figures 5 and 6. Figure 5 shows a cross-sectional view of the glycophorin A trans-

Table 1: Interhelical Distances and Restraints from Solid-State NMR Measurements of the Glycophorin A Transmembrane Dimer

helix 1	helix 2	interhelical distance (Å)	restraint (Å)
Gly79 ($^{13}CH_2$)	Gly79 ($^{13}C{=}O$)	4.1 (5.2)[a]	3.8−4.4
Ile76 ($^{13}C{=}O$)	Gly79 ($^{13}CH_2$)	4.8 (5.3)	4.5−5.1
Gly83 ($^{13}CH_2$)	Gly83 ($^{13}C{=}O$)	4.3 (5.2)	4.0−4.6
Gly83 ($^{13}CH_2$)	Val80 ($^{13}C{=}O$)	4.2 (4.5)	3.9−4.5
Gly79 ($^{13}C{=}O$)	Val80 ($^{13}CH_3$)	4.0 (2.8)	3.7−4.3
Gly83 ($^{13}C{=}O$)	Val84 ($^{13}CH_3$)	4.0 (3.4)	3.7−4.3

[a] Distances in parentheses (in Å) were obtained from the model of the glycophorin A dimer (PDB code 1AFO) based on solution NMR NOE restraints (*23*).

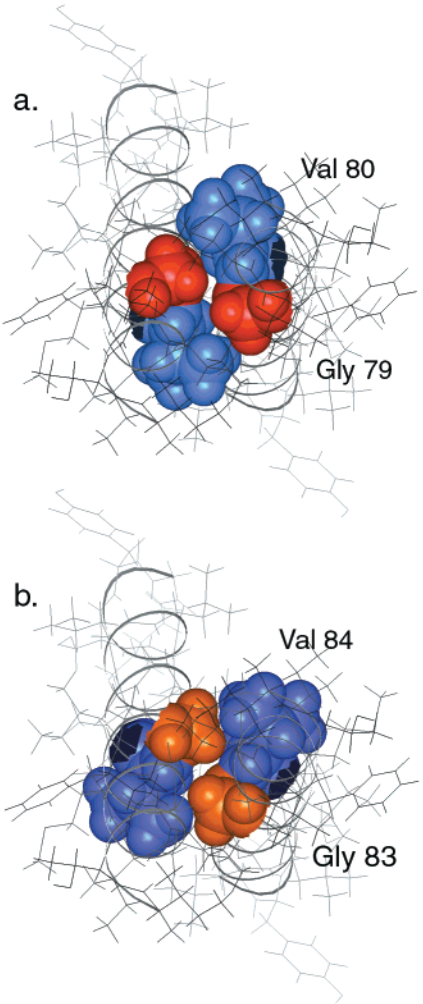

FIGURE 5: Structural model of the glycophorin A transmembrane dimer. View down the dimer axis showing the close packing of Gly79−Gly79 (a) and Gly83−Gly83 (b). The dimer model was obtained using the computational search algorithm developed by Brünger and Adams (*22*) and the following NMR restraints: Gly79 ($^{13}CH_2$)···Gly79 ($^{13}C{=}O$), 4.1 Å; Gly83 ($^{13}CH_2$)···Gly83 ($^{13}C{=}O$), 4.3 Å; Gly79 ($^{13}CH_2$)···Ile76 ($^{13}C{=}O$), 4.8 Å; Gly83 ($^{13}CH_2$)···Val80 ($^{13}C{=}O$), 4.3 Å; Gly79 ($^{13}C{=}O$)···Val80 ($^{13}CH_3$), 4.0 Å; Gly83 ($^{13}C{=}O$)···Val84 ($^{13}CH_3$), 4.0 Å.

membrane dimer looking down the dimer axis and highlights the close packing of Gly79−Gly79 (Figure 5a) and Gly83−Gly83 (Figure 5b). The glycine residues are in close van der Waals contact with one another across the dimer interface. Gly79 and Gly83 are also closely packed with Val80 and Val84, respectively, as determined previously by MAS NMR (*8*).

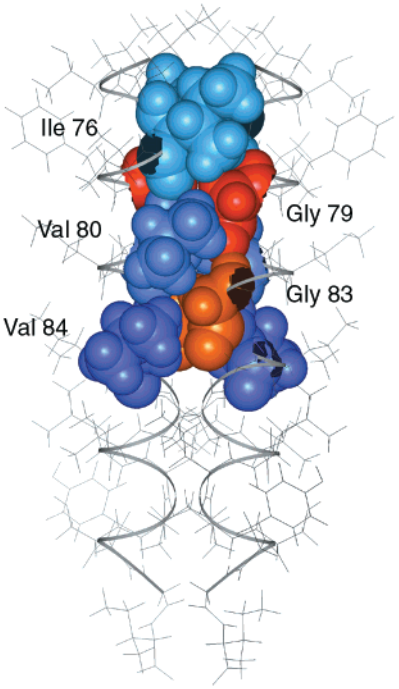

FIGURE 6: Structural model of the glycophorin A transmembrane dimer. View along the dimer interface highlighting Gly79, Gly83, Ile76, Val80, and Val84. The β-branched amino acids are locked in the gauche$^+$ conformation and form a ridge that packs against the surface formed by Gly79 and Gly83.

Figure 6 shows the transmembrane dimer viewed along the dimer axis. This orientation highlights the three β-branched residues, Ile76, Val80, and Val84, which form a ridge of amino acids that pack along the groove created by Gly79and Gly83. The conformation and intrahelical packing of these residues are defined by the χ^1 torsion angle. For all three β-branched side chains, the conformation corresponds to the dominant rotamer observed when these residues occur in α-helices (*15*). Packing of the β-methyl group of Ile76 against Val80 and of the β-methyl group of Val80 against Val84 is thought to provide helix stabilizing interactions (*16*, *17*).

The defining feature of the structure is the closely packed glycine residues. In an analysis of the packing of membrane proteins, we recently found that the transmembrane helices in membrane proteins have higher average packing values (0.441) than helices in soluble proteins (0.414). The tight packing can be attributed in large part to small residues (Gly, Ser, and Thr) which are among the most tightly packed in membrane protein interiors (*2*). The average packing value for the seven residues comprising the dimerization motif in glycophorin A is 0.44, with the highest individual packing values being associated with Gly79 (0.55) and Gly83 (0.57). The packing data are consistent with the mutational studies on glycophorin A dimerization which show that dimer formation is the most sensitivity to the residue at position 83 and is completely disrupted even by the G83A substitution (*5*). The close glycine−glycine packing is similar to that observed in the activated *neu* receptor transmembrane domain (S. Smith, unpublished results). The tight glycine packing is also consistent with the observation that glycine residues appear to reside on the same face of transmembrane α-helices (*17*−*19*). More generally, we and others have found that there is a rough correlation between residue size and their

Table 2: Interhelical Distances and Restraints from Solution NMR Measurements of the Glycophorin A Transmembrane Dimer[a]

helix 1	helix 2	interhelical distance (Å)	restraint (Å)
Val80 (Hγ2)	Gly79 (Hn)	4.1 (4.9)[b]	2.5−5.0
Val84 (Hγ2)	Thr87 (Hγ1)	2.1 (2.4)	2.1−2.7
Val84 (Hγ2)	Gly83 (Hα)	2.4 (2.4)	2.1−3.0
Thr87 (Hγ2)	Ile88 (Hn)	4.2 (2.9)	2.2−4.5
Ile88 (Hγ1)	Thr87 (Hγ2)	3.1 (2.5)	2.2−3.2

[a] Distances and restraints derived from observed solution NMR NOEs (*23*). [b] Distances in parentheses (Å) were obtained from the model of the glycophorin A dimer based on MAS NMR distance measurements.

normalized occurrence in helix interfaces (*2*, *3*, *19*).

The structure of the glycophorin dimer in membranes presented here can be compared with the structure in detergent micelles proposed on the basis of interhelical NOE correlations (*9*) and modeling (*20*). The major difference between the structures is a rotation of the interacting helical faces by ∼25°. This places the glycine residues in direct van der Waals contact in the membrane structure and allows Thr87 to hydrogen bond across the dimer interface (S. Smith, unpublished results). The membrane structure is consistent with the interhelical NOE constraints (*23*) used previously to model the dimer (Table 2). However, the detergent structure is *not* consistent with the high-resolution constraints established by MAS NMR measurements (Table 1). The ∼35° crossing angle of the helices in the membrane structure is reduced relative to that in detergents (*9*). As a result, the differences between the detergent and membrane structures may reflect the larger number of more accurate distance constraints provided by MAS NMR or may reflect the environmental differences between detergent micelles and membrane bilayers. For instance, the smaller crossing angle in the membrane structure may result from forces imposed by the "two-dimensional" membrane bilayer to orient the transmembrane helices parallel to the membrane normal.

These results highlight the importance of the glycophorin A transmembrane dimer as a simple model system for defining the key structural features of helix association in membrane bilayers. The general model which emerges from an analysis of helix−helix interactions in glycophorin A and membrane proteins with known crystal structures is that small residues frequently occur in helix interfaces and allow close helix packing of transmembrane helices (*2*, *3*). This packing architecture is fundamentally different from that seen in helical soluble proteins. In membrane proteins, the close packing provides increased stability through dipolar interactions involving the polar peptide backbone (*3*) and facilitates the formation of interhelical hydrogen bonds. In particular, Ser and Thr, the most abundant polar residues in transmembrane helices, do not readily form interhelical hydrogen bonds in the context of a "leucine-zipper" motif (*24*) but are observed to form interhelical hydrogen bonds in the region of small residues in the crystal structures of membrane proteins (M. Eilers and S. Smith, unpublished results). These polar interactions then drive the association of hydrophobic helices in a hydrophobic membrane environment (*24*).

REFERENCES

1. Popot, J. L., and Engelman, D. M. (2000) *Annu. Rev. Biochem. 69*, 881−922.
2. Eilers, M., Shekar, S. C., Shieh, T., Smith, S. O., and Fleming, P. J. (2000) *Proc. Natl. Acad. Sci. U.S.A. 97*, 5796−5801.
3. Javadpour, M. M., Eilers, M., Groesbeek, M., and Smith, S. O. (1999) *Biophys. J. 77*, 1609−1618.
4. Bormann, B. J., Knowles, W. J., and Marchesi, V. T. (1989) *J. Biol. Chem. 264*, 4033−4037.
5. Lemmon, M. A., Flanagan, J. M., Treutlein, H. R., Zhang, J., and Engelman, D. M. (1992) *Biochemistry 31*, 12719−12725.
6. Lemmon, M. A., Flanagan, J. M., Hunt, J. F., et al. (1992) *J. Biol. Chem. 267*, 7683−7689.
7. Treutlein, H. R., Lemmon, M. A., Engelman, D. M., and Brunger, A. T. (1992) *Biochemistry 31*, 12726−12732.
8. Smith, S. O., and Bormann, B. J. (1995) *Proc. Natl. Acad. Sci. U.S.A. 92*, 488−491.
9. MacKenzie, K. R., Prestegard, J. H., and Engelman, D. M. (1997) *Science 276*, 131−133.
10. Metz, G., Wu, X., and Smith, S. O. (1994) *J. Magn. Reson., Ser. A 110*, 219−227.
11. Bennett, A. E., Rienstra, C. M., Auger, M., Lakshmi, K. V., and Griffin, R. G. (1995) *J. Chem. Phys. 103*, 6951−6958.
12. Peersen, O. B., Groesbeek, M., Aimoto, S., and Smith, S. O. (1995) *J. Am. Chem. Soc. 117*, 7228−7237.
13. Fleming, K. G., Ackerman, A. L., and Engelman, D. M. (1997) *J. Mol. Biol. 272*, 266−275.
14. Fisher, L. E., Engelman, D. M., and Sturgis, J. N. (1999) *J. Mol. Biol. 293*, 639−651.
15. Dunbrack, R. L., Jr., and Karplus, M. (1993) *J. Mol. Biol. 230*, 543−574.
16. Walther, D., and Argos, P. (1996) *Protein Eng. 9*, 471−478.
17. Senes, A., Gerstein, M., and Engelman, D. M. (2000) *J. Mol. Biol. 296*, 921−936.
18. Arkin, I. T., and Brunger, A. T. (1998) *Biochim. Biophys. Acta 1429*, 113−128.
19. Russ, W. P., and Engelman, D. M. (2000) *J. Mol. Biol. 296*, 911−919.
20. MacKenzie, K. R., and Engelman, D. M. (1998) *Proc. Natl. Acad. Sci. U.S.A. 95*, 3583−3590.
21. Small, D. M. (1986) Phospholipids, in *The physical chemistry of lipids* (Small, D. M., Ed.) p 482, Plenum Press, New York.
22. Adams, P. D., Engelman, D. M., and Brunger, A. T. (1996) *Proteins 26*, 257−261.
23. Mackenzie, K. M. (1996) Structure determination of the dimeric membrane spanning domain of glycophorin A in detergent micelles by triple resonance nuclear magnetic resonance spectroscopy, Ph.D. Thesis, Yale University, New Haven, CT.
24. Gratkowski, H., Lear, J. D., and DeGrado, W. F. (1996) *Proc. Natl. Acad. Sci. U.S.A. 98*, 880−885.

BI010357V